Inorg. Chem. **2009**, *48*, 1038−1044

Effects of Hyperconjugation on the Electronic Structure and Photoreactivity of Organic Sulfonyl Chlorides

Vlad Martin-Diaconescu and Pierre Kennepohl*

The University of British Columbia, Department of Chemistry, Vancouver, British Columbia V6T 1Z1

Received August 30, 2008

The electronic structure of organic sulfonyl compounds of the form RSO_2G (G = −Cl, −OH, $-CH_3$) is investigated to evaluate the effect of aryl R groups on photocleavage of the S−G bond. Sulfur K-edge X-ray absorption spectroscopy (XAS) provides a direct measure of the empty low-lying molecular orbitals in these complexes and, in combination with DFT calculations, a detailed description of the bonding in these compounds. The presence of an aryl group bound to the sulfonyl moiety has a significant impact on the spectroscopy and electronic structure of the site. The analysis suggests that the SCl_{σ^*} orbital is significantly affected by mixing with the aryl π^* manifold. This mixing is dependent upon the nature of G and is most pronounced in the sulfonyl chlorides, where the energy of the SCl_{σ^*} orbital is lowered by ∼0.5 eV. The observed mixing is best described as excited-state hyperconjugation of the aryl π system into the SCl_{σ^*} orbital. The magnitude of the effect can be estimated directly from the S K-edge XAS spectra. These results are discussed in relation to the observed photochemistry of RSO_2Cl, which is significantly enhanced when R = aryl as compared to alkyl substituents.

Introduction

p-Toluene sulfonyl chloride (**1a**) has been described as a universal initiator in living radical polymerization reactions due to its ability to catalyze the polymerization of styrene, methacrylates, and acrylates[1] with little apparent impact on the reactivity by the substituents on the phenyl group.[2] This behavior has generally been attributed to a lack of hyperconjugation on the part of the sulfonyl moiety with the phenyl ring in the *p*-toluene sulfonyl radical intermediate,[2,3] even though there is both experimental and computational evidence for hyperconjugation in sulfonyl compounds.[4] The sulfonyl radical intermediate involved in the polymerization reaction is generated from cleavage of the S−Cl bond, which can be achieved via metal reduction, thermolysis, or photoirradiation.[2,3,5] We recently began to explore the electronic structure of **1a** and related sulfonyl species to better define the importance of hyperconjugation and its impact on sulfonyl radical generation and subsequent radical polymerization.

X-ray absorption spectroscopy (XAS) at the sulfur K-edge was used to characterize the electronic structure of the sulfonyl center. S K-edge XAS spectra are dominated by the ionization edge ($\infty \leftarrow S_{1s}$, observed as a discontinuity in the spectrum) as well as electric dipole-allowed transitions between the localized S_{1s} atomic orbital and unoccupied or partially unoccupied molecular orbitals (MOs) with significant S 3p character.[6] Importantly, the low-lying empty valence molecular orbitals that serve as potential acceptor orbitals for these pre-edge XAS transitions correspond to the antibonding counterparts of each of the chemical bonds to sulfur within the molecule of interest. These bound-state transitions, therefore, can provide direct information regarding the nature of the bonding to that particular atom.[7]

The series of compounds of the form RSO_2G (Scheme 1) was investigated to probe the properties of the SG bond (G = −Cl, −OH, $-CH_3$/$-CH_2CH_3$) as a function of the nature

* To whom correspondence should be addressed. E-mail: pierre@chem.ubc.ca.

(1) Percec, V.; Kim, H. J.; Barboiu, B. *Macromolecules* **1997**, *30*, 8526–8528.
(2) Percec, V.; Barboiu, B.; Kim, H. J. *J. Am. Chem. Soc.* **1998**, *120*, 305–316.
(3) Orochov, A.; Asscher, M.; Vofsi, D. *J. Chem. Soc. B, Phys. Org.* **1969**, 255–259.
(4) Fehnel, E. A.; Carmack, M. *J. Am. Chem. Soc.* **1950**, *72*, 1292–1297. Denehy, E.; White, J. M.; Williams, S. J. *Inorg. Chem.* **2007**, *46*, 8871–8886.
(5) Kharasch, M. S.; Zavist, A. F. *J. Am. Chem. Soc.* **1951**, *73*, 964–967.
(6) Glaser, T.; Hedman, B.; Hodgson, K. O.; Solomon, E. I. *Acc. Chem. Res.* **2000**, *33*, 859–868.

10.1021/ic801665f CCC: $40.75
Published on Web 12/31/2008

Scheme 1. Complementary Series of Aryl (a) and Alkyl (b) Model Compounds of the Form RSO_2G, where G = −Cl (**1**), −OH (**2**), and $-CH_3$/$-CH_2CH_3$ (**3**)

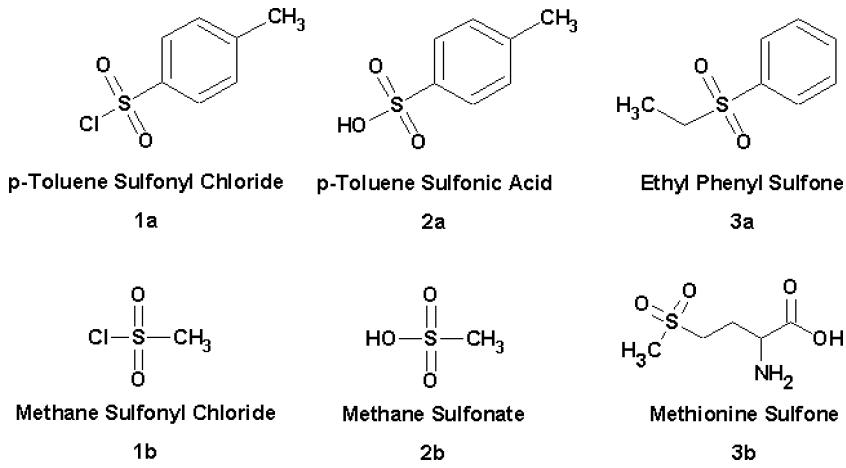

Scheme 2. Sulfonyl Chloride Photocleavage Reaction, where R = Alkyl, *p*-Tolyl

$$RSO_2Cl \xrightarrow{h\nu} [RSO_2Cl]^* \longrightarrow RSO_2^{\bullet} + Cl^{\bullet}$$

of the R group. Specifically, the effect of the π system is explored by comparing aryl (**a**, R = *p*-XC_6H_4-, X = H/CH_3) vs alkyl (**b**) compounds. Photocleavage of the SCl bond in **1a,b** (Scheme 2) was also explored to investigate the correlation between observed photochemical reactivity and the hyperconjugation effects observed in the same compounds. Density functional (DFT) calculations were employed to assist in the assignment of the XAS data and probe the bonding around the sulfur center. The effect of orbital mixing in the aryl compounds is explored, and a quantitative estimate of hyperconjugation in the photoexcited state of **1a** is obtained. The implications of this hyperconjugative effect on photocleavage of the S−Cl bond are discussed.

Results

S K-Edge XAS Spectroscopy. The S K-edge XAS spectra of **1a,b**, **2a,b**, and **3a,b** are shown in Figures 1, 2, and 3, respectively. Differences in the pre-edge region of the spectra are clearly observed as a function of the nature of substituent G and the nature of the R group. In all cases, the aryl compounds (**1a**, **2a**, and **3a**) exhibit additional features not present in the spectra of their alkyl counterparts (**1b**, **2b**, and **3b**). Most notably, **3a** exhibits a shoulder (∼2478.6 eV, Figure 3) as compared to **3b**; the main absorption feature of the spectrum is also at slightly higher energy (2480.6 eV in **3a** vs 2480.1 eV in **3b**). Compound **1a** has peaks at 2477.4 and 2481.2 eV in addition to a shoulder at 2479.6 eV, whereas **1b** has only two peaks at 2477.6 and 2480.9 eV (see Figure 1). Lastly, **2a** has three features (at 2479.9, 2481.7, and 2483.9 eV), and **2b** exhibits only a main peak at 2481.3 eV and a shoulder at 2483.1 eV (see Figure 2). The presence of an aromatic ring bound to the sulfur atom therefore has a significant effect on the energy distribution of S 3p character over the final states either through the presence of additional transitions or through energy redistribution of existing transitions in alkyl compounds.

DFT Calculations and Spectroscopic Assignments. To understand the nature of the transitions in the S K-edge XAS spectra and evaluate the nature of the effect of the aryl substituent the S K-edge spectra were simulated using TD-

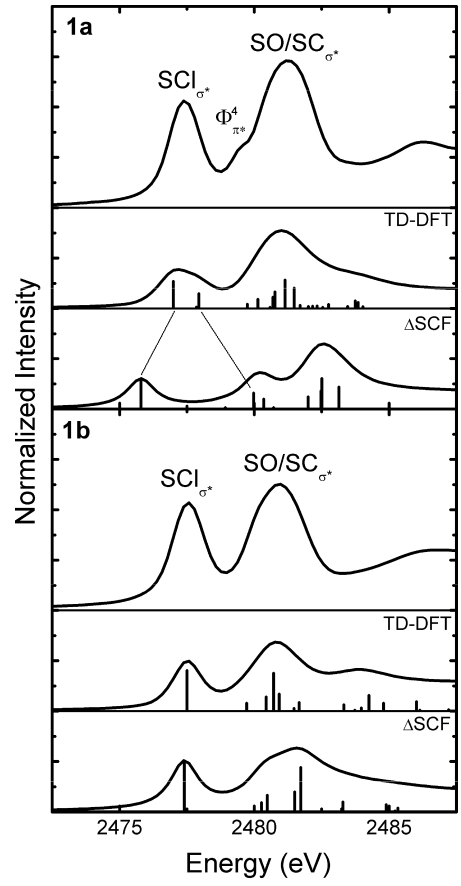

Figure 1. Sulfur K-edge XAS spectra of **1a** (top) and **1b** (bottom) including TD-DFT and ΔSCF-simulated spectra. Simulations include bars representing calculated energies and intensities of the first 10 calculated transitions and a simulated spectrum derived from Gaussian convolution of the first 20 calculated transitions. See text for details.

(7) de Groot, F. M. F. *Inorg. Chim. Acta* **2008**, *361*, 850–856. Jalilehvand, F. *Chem. Soc. Rev.* **2006**, *35*, 1256–1268. Neese, F.; Hedman, B.; Hodgson, K. O.; Solomon, E. I. *Inorg. Chem.* **1999**, *38*, 4854–4860. Rose, K.; Shadle, S. E.; Eidsness, M. K.; Kurtz, D. M.; Scott, R. A.; Hedman, B.; Hodgson, K. O. Solomon, E. I. *J. Am. Chem. Soc.* **1998**, *120*, 10743–10747. Solomon, E. I.; Hedman, B.; Hodgson, K. O.; Dey, A.; Szilagyi, R. K. *Coord. Chem. Rev.* **2005**, *249*, 97–129.

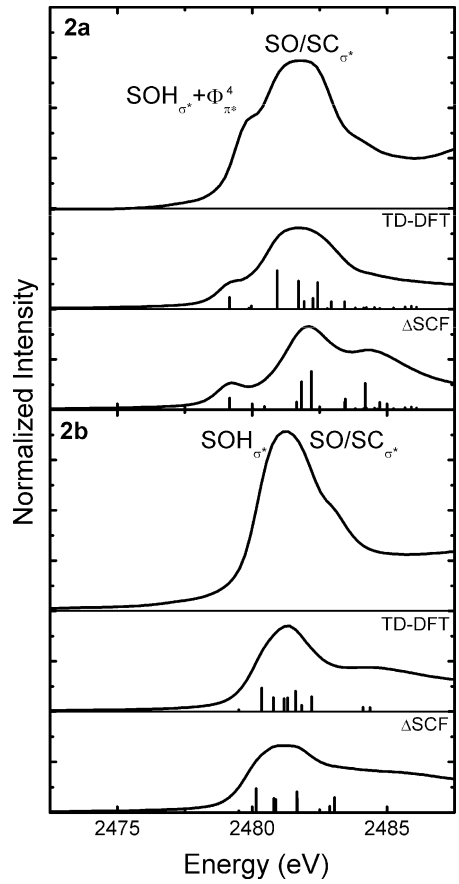

Figure 2. Sulfur K-edge XAS spectra of **2a** (top) and **2b** (bottom) including TD-DFT and ΔSCF-simulated spectra. Simulations include bars representing calculated energies and intensities of the first 10 calculated transitions and a simulated spectrum derived from Gaussian convolution of the first 20 calculated transitions. See text for details.

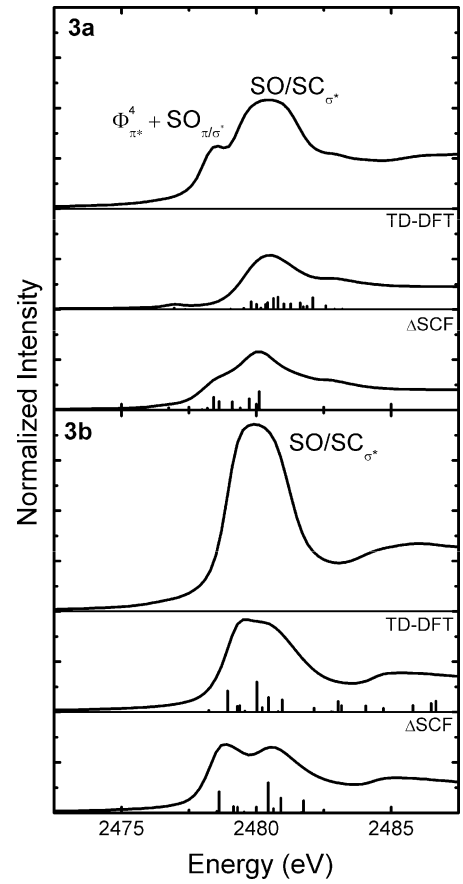

Figure 3. Sulfur K-edge XAS spectra of **3a** (top) and **3b** (bottom) including TD-DFT and ΔSCF-simulated spectra. Simulations include bars representing calculated energies and intensities of the first 10 calculated transitions and a simulated spectrum derived from Gaussian convolution of the first 20 calculated transitions. See text for details.

DFT calculations. Descriptions of the assignments of the lowest energy transitions for each TD-DFT calculation are given in Tables 1−6.[8] The pre-edge region of the calculated spectra for the alkyl compounds (**1b**, **2b**, and **3b**) are in reasonable agreement with the experimental spectra. In all cases, the most intense feature of the spectrum is dominated by the σ^* acceptor states for the S−C and S=O bonds in the RSO_2 molecular fragment. In **1b** an additional feature is observed, which corresponds to the low-energy $SCl_{\sigma^*} \leftarrow S_{1s}$ transition. For the aryl compounds, however, the TD-DFT simulation for **2a** is in reasonable agreement with the experimental data, whereas **1a** and **3a** show significant differences between the calculated and experimental spectra. The TD-DFT simulation for **1a** predicts a high-energy shoulder on the peak at 2477.4 eV and does not properly account for the shoulder at 2479.6 eV. In the case of **3a** TD-DFT fails to account for the feature at 2478.6 eV.

Given that TD-DFT calculations do not inherently account for electronic relaxation (i.e., electronic changes in the excited state) in the excited states, we recalculated the transition energies using the Slater transition state ΔSCF approach[9] to explore whether relaxation effects could account for the observed discrepancies with the experimental spectra. Oscillator strengths from the TD-DFT calculations were retained to generate ΔSCF-based simulations (see Figures 1, 2, and 3 for simulations and Tables 1−6 for calculated ΔSCF corrections). The ΔSCF approach can overestimate relaxation shifts but allows for an exploration of which transitions are most susceptible to relaxation effects. In each case, the energy distribution of the excited states changes

Table 1. Sulfur K-Edge DFT-Calculated Transitions for **1a** with Major Contributors Listed First[a]

transition	assignment (primary + others)	TD-DFT energies (eV)	ΔSCF (eV)	f
1	SCl_{σ^*}, $\Phi^4_{\pi^*}$, SO_{π^*}	2476.99	0.0	2.3×10^{-3}
2	$\Phi^5_{\pi^*}$	2477.85	+2.3	1.1×10^{-4}
3	$\Phi^4_{\pi^*}$, SO_{σ^*},SCl_{σ^*}	2477.94	+3.2	1.3×10^{-3}
4	$C_\phi S_{\sigma^*}$, SO_{σ^*}	2479.74	+1.8	3.6×10^{-4}
5	SO_{σ^*}	2480.13	+1.4	7.9×10^{-4}
6	SO_{π^*}, SO_{σ^*}, Φ_{o^*}	2480.59	+1.3	1.0×10^{-4}
7	Φ_{o^*}	2480.69	+2.5	9.6×10^{-4}
8	Φ_{o^*},	2480.76	+2.9	1.4×10^{-3}
9	SO_{σ^*}, SO_{π^*}, Φ_{o^*}	2481.14	+2.6	2.4×10^{-3}

[a] ΔSCF energies are shifts from the calculated TD-DFT transition energies referenced to the lowest energy transition.

(8) The XAS of **2b** was simulated with transitions from the TD-DFT of $(CH_3)SO_2OH$, and **3b** was simulated with transitions from the TD-DFT of $(CH_3)_2SO_2$.

(9) Schwarz, K. *Chem. Phys.* **1975**, *7*, 100–107. Sen, K. D. *J. Phys. Chem. B* **1978**, *11*, L577−L578. Gopinathan, M. S. *J. Phys. Chem. B* **1979**, *12*, 521–529. Triguero, L.; Pettersson, L. G. M.; Agren, H. *J. Phys. Chem. A* **1998**, *102*, 10599–10607. Triguero, L.; Pettersson, L. G. M.; Agren, H. *Phys. Rev. B* **1998**, *58*, 8097–8110.

Table 2. Sulfur K-Edge DFT-Calculated Transitions for **1b** with Major Contributors Listed First[a]

transition	assignment (primary, others)	TD-DFT energies (eV)	ΔSCF (eV)	f
1	SCl_{σ^*}, SO_{π^*}	2477.50	0.00	3.8×10^{-3}
2	SC_{σ^*}, SO_{σ^*}	2479.72	+0.66	7.2×10^{-4}
3	SC_{σ^*}, SO_{σ^*}	2480.44	+0.18	1.3×10^{-3}
4	SC_{σ^*}, SO_{π^*}	2480.72	+1.12	3.5×10^{-4}
5	$SO_{\sigma^*}CH_{\sigma^*}$	2480.92	+0.70	1.6×10^{-3}
6	CH_{σ^*}, SO_{σ^*}	2481.48	+1.84	2.4×10^{-4}
7	CH_{σ^*}, SO_{σ^*}	2481.67	+1.68	7.9×10^{-4}

[a] ΔSCF energies are shifts from the calculated TD-DFT transition energies referenced to the lowest energy transition.

Table 3. Sulfur K-edge DFT-Calculated Transitions for **2a** with Major Contributors Listed First[a]

transition	assignment (primary, others)	TD-DFT energies (eV)	ΔSCF (eV)	f
1	$\Phi^4_{\pi^*}$, SO_{π^*}, SOH_{σ^*}	2479.16	0.00	1.3×10^{-3}
2	$\Phi^5_{\pi^*}$	2479.87	+0.16	1.0×10^{-4}
3	$\Phi^4_{\pi^*}$, SOH_{σ^*}, SO_{σ^*}	2479.97	+0.49	3.6×10^{-4}
4	SO_{π/σ^*}	2480.93	+1.27	4.3×10^{-3}
5	SO_{π/σ^*},$\Phi^4_{\pi^*}$	2481.71	+0.11	3.2×10^{-3}
6	SC_{σ^*}, SO_{π^*}	2481.92	−0.28	8.7×10^{-4}
7	SC_{σ^*}, SO_{π^*}, OH_{σ^*}	2482.25	+1.21	1.2×10^{-3}
8	SC_{σ^*}, SO_{π^*}, OH_{σ^*}	2482.43	+1.76	3.0×10^{-3}
9	Φ_{σ^*}	2482.78	+1.86	7.4×10^{-5}

[a] ΔSCF energies are shifts from the calculated TD-DFT transition energies referenced to the lowest energy transition.

Table 4. Sulfur K-Edge DFT-Calculated Transitions for **2b** with Major Contributors Listed First[a]

transition	assignment (primary, others)	TD-DFT energies (eV)	ΔSCF (eV)	f
1	SOH_{σ^*}, SC_{σ^*}, SO_{σ^*}	2479.50	0.00	2.0×10^{-4}
2	SO_{π^*}, SC_{σ^*}	2480.35	−0.21	2.7×10^{-3}
3	SC_{σ^*}, SOH_{σ^*}	2480.78	+0.02	1.6×10^{-3}
4	SC_{σ^*}, SO_{π^*}	2481.18	−0.30	1.5×10^{-3}
5	SO_{π/σ^*}, SO_{σ^*}	2481.31	+0.37	1.6×10^{-3}
6	CH_{σ^*}, SO_{σ^*}	2481.61	+0.05	2.3×10^{-3}
7	CH_{σ^*}, SO_{σ^*}	2481.83	+1.04	7.1×10^{-4}

[a] ΔSCF energies are shifts from the calculated TD-DFT transition energies referenced to the lowest energy transition.

Table 5. Sulfur K-Edge DFT-Calculated Transitions for **3a** with Major Contributors Listed First[a]

transition	assignment (primary, others)	TD-DFT energies (eV)	ΔSCF (eV)	f
1	$\Phi^4_{\pi^*}$	2476.95	0.00	1.8×10^{-4}
2	$\Phi^5_{\pi^*}$	2477.36	+0.85	3.6×10^{-6}
3	SC_{σ^*},$C_\phi S_{\sigma^*}$	2479.04	−0.86	4.1×10^{-5}
4	SC_{σ^*},$C_\phi S_{\sigma^*}$	2479.53	−1.15	1.4×10^{-4}
5	SO_{π^*},SO_{σ^*},SC_{σ^*},$C_\phi S_{\sigma^*}$	2479.81	−1.20	1.0×10^{-3}
6	SO_{π^*},SO_{σ^*},SC_{σ^*},$C_\phi S_{\sigma^*}$	2480.01	−1.19	6.8×10^{-4}
7	SO_{σ^*}, SO_{π^*}	2480.17	−0.57	1.6×10^{-4}
8	SO_{σ^*}, SO_{π^*}	2480.34	−1.03	6.7×10^{-4}
9	CH_{σ^*}	2480.42	−0.49	8.8×10^{-4}

[a] ΔSCF energies are shifts from the calculated TD-DFT transition energies referenced to the lowest energy transition.

due to final state relaxation. For the alkyl compounds we find that the most intense feature of the spectrum broadens significantly as a result of relaxation; in the case of **3b**, the feature splits into two peaks.

In general, relaxation effects are more pronounced for the aryl compounds. The effect is least pronounced in **2a**, where the overall shape of the simulated spectrum remains unchanged (see Figure 2). The effect is larger in **3a**, where the ΔSCF simulation more accurately reflects the experimental

Table 6. Sulfur K-Edge DFT-Calculated Transitions for **3b** with Major Contributors Listed First[a]

transition	assignment (primary, others)	TD-DFT energies (eV)	ΔSCF (eV)	f
1	SC_{σ^*}	2478.53	0.00	1.9×10^{-4}
2	SC_{σ^*}	2479.24	−0.62	2.4×10^{-3}
3	CH_{σ^*}, SO_{σ^*}	2479.59	−0.30	6.2×10^{-4}
4	SC_{σ^*}, SO_{π^*}	2479.69	−0.54	7.0×10^{-4}
5	CH_{σ^*}, SO_{σ^*}	2479.87	−0.33	1.0×10^{-4}
6	SO_{π^*}, CH_{σ^*}	2480.31	+0.13	3.4×10^{-3}
7	CH_{σ^*}, SO_{σ^*}	2480.52	+0.12	4.7×10^{-4}
8	SO_{σ^*}, CH_{σ^*}	2480.75	+0.16	1.7×10^{-3}

[a] ΔSCF energies are shifts from the calculated TD-DFT transition energies referenced to the lowest energy transition.

spectrum. The energies for transitions 5 and 6 of **3a** are shifted to lower energy by ∼1.1 eV and help account for the feature at 2478.6 eV. The impact is even more substantial for **1a**, where relaxation strongly affects the three lowest energy transitions (see Table 1). The splitting of transitions 1 from 2/3 increases significantly, pushing the latter transitions closer to the main feature at 2481.2. The distribution of intensity in the ΔSCF simulation more accurately describes the observed intensity pattern and suggests that transitions 2/3 are responsible for the experimentally observed shoulder at 2479.6 eV, a shoulder that is not accounted for in the TD-DFT simulation.

On the basis of the combination of the TD-DFT and ΔSCF results a general assignment of the S K-edge XAS spectra is possible for each of the complexes as labeled in Figures 1, 2, and 3. The sulfonyl chlorides (**1a,b**, Figure 1) both have two main features: the low-energy $SCl_{\sigma^*} \leftarrow S_{1s}$ transition and a higher energy feature corresponding to the $SO_{\sigma^*} \leftarrow S_{1s}$ and $SC_{\sigma^*} \leftarrow S_{1s}$ transitions. The aryl species has an additional shoulder which corresponds to the $\Phi^4_{\pi^*} \leftarrow S_{1s}$ transition. This $\Phi^4_{\pi^*}$ acceptor orbital is one of two low-lying π^* orbitals of the tolyl ring ($\Phi^4_{\pi^*}$ and $\Phi^5_{\pi^*}$) and corresponds to that orbital which has the largest contribution on the carbon atom bound to the sulfonyl moiety (see Figure 5). This allows for mixing with the SCl_{σ^*} final state, through which intensity is borrowed, thus allowing this transition to be visible in the S K-edge XAS spectrum.

The sulfonic acids (**2a,b**, Figure 2) do *not* show a similar intense pre-edge feature relating to the SG_{σ^*} since the energy of the SOH_{σ^*} acceptor orbital is at much higher energy than the SCl_{σ^*}. However, as with the sulfonyl chlorides, aryl substitution causes the appearance of an additional feature in the S K-edge spectrum. The main feature in both **2a** and **2b** corresponds to the $SO_{\sigma^*}/SC_{\sigma^*} \leftarrow S_{1s}$ transitions, which are ∼0.5 eV higher in energy than the corresponding transitions in **1a** and **1b**. The low-energy shoulder observed in **2a** is attributed to the $SOH_{\sigma^*} \leftarrow S_{1s}$ transition, which has been lowered in energy through mixing with the $\Phi^4_{\pi^*}$ orbital of the aryl group. The presence of this feature therefore results from mixing of the SOH bond with the π network of the aryl group.

A similar effect is observed when comparing **3a** and **3b**, although the assignment differs (Figure 3). As with all of the sulfonyls, the main feature is attributed to a combination of $SO_{\sigma^*} \leftarrow S_{1s}$ and $SC_{\sigma^*} \leftarrow S_{1s}$ transitions. In these complexes the main feature is ∼0.5 eV lower in energy than the

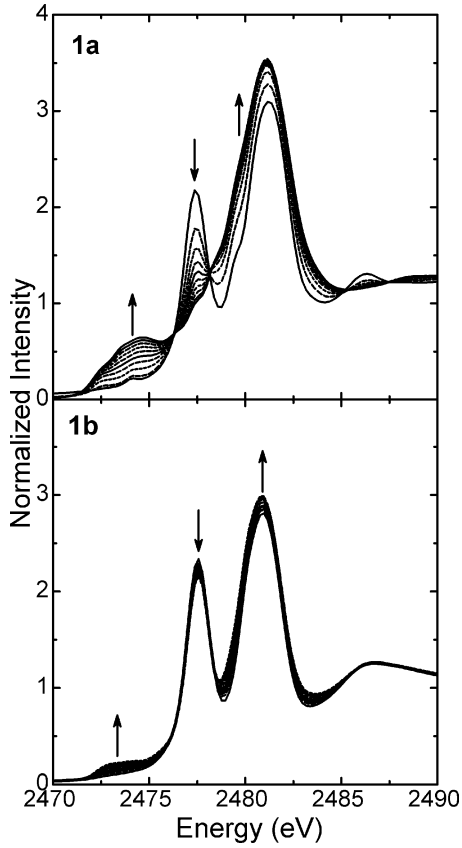

Figure 4. X-ray absorption spectra of **1a** (top) and **1b** (bottom) irradiated with a 75 W Xe Arc lamp under anaerobic conditions. Scans taken every ~5 min with continuous irradiation.

corresponding transitions in **1a,b**. The low-energy shoulder observed in **3a** results from the $\Phi^4_{\pi^*}$ final state, which gains intensity in this case from the SO_{σ^*} final states, which are closer in energy than in the other aryl compounds.

Photocleavage Reactions. We followed the S−Cl bond photocleavage reaction by S K-edge XAS (Figure 4) to confirm differences in the susceptibility of bond cleavage in **1a** and **1b** and explore the nature of the resultant photoproducts. Our data confirm that photoirradiation of both compounds with a Xe arc lamp results in cleavage of the S−Cl bond (as observed from the loss of the corresponding $SCl_{\sigma^*} \leftarrow S_{1s}$ feature) and formation of *lower energy* pre-edge features. Photoconversion to radical products is significantly increased in **1a**.

Discussion

The assignment of the S K-edge XAS spectra of these compounds provides an opportunity to explore the electronic structure of these species and thus provides insight into their reactivity, especially as it pertains to the use of sulfonyl chlorides as radical initiators in polymerization. Most importantly, our data confirm that the presence of an aromatic group directly bound to the sulfonyl moiety enables direct electronic coupling and should thus have an impact on reactivity. The presence of new features in the S K-edge XAS spectrum attributable to the presence of aryl π^* final states (specifically from the $\Phi^4_{\pi^*}$ acceptor orbital) clearly demonstrates mixing with the S 3p manifold.

The nature of the interactions observed in the S K-edge spectra provides some insights into the nature of bonding in these systems. In the alkyl compounds (**1b**−**3b**) the excited final states suggest a specific ordering of the empty valence orbitals in these species, i.e., $E(SG_{\sigma^*}) < E(SR_{\sigma^*}) < E(SO_{\pi^*}) < E(SO_{\sigma^*})$. The splitting of these final states, however, is relatively small in **2b** and **3b** such that one observes a single intense broad peak as the main feature. By contrast, the $SCl_{\sigma^*} \leftarrow S_{1s}$ transition in **1b** is well separated at lower energy, accounting for the weaker intensity of the main feature (relative to **2b** and **3b**) and the presence of the pre-edge feature ~3 eV below the main peak. The situation differs in the aryl compounds, where the ordering of the $SR_{\sigma^*} \leftarrow S_{1s}$ and $SO_{\sigma^*} \leftarrow S_{1s}$ transitions switches such that $E(SG_{\sigma^*}) < E(SO_{\pi^*}) < E(SO_{\sigma^*}) < E(SR_{\sigma^*})$. As with the alkyl compounds, the energy splitting of the SO and SC antibonding orbitals is quite small such that the features are unresolved in the experimental spectra. The reordering of the SR_{σ^*} and SO_{σ^*} final states in the aryl compounds reflects the greater strength of the S−C(sp^2) bond.[10] The stronger S−C bond leads to greater destabilization of the SC_{σ^*} orbital and thus a higher $SC_{\sigma^*} \leftarrow S_{1s}$ transition energy. This is consistent with the fact that the main features of the aryl compounds are all ~0.4 eV higher in energy than their alkyl counterparts, presumably due to the increase in energy of the SC_{σ^*} acceptor orbital.

Aryl substitution, however, has a greater impact on bonding than simply changing the strength of the SR_{σ^*} bond. Most notably, the aryl group presents two low-lying π^* orbitals ($\Phi^4_{\pi^*}$ and $\Phi^5_{\pi^*}$) which can mix and redistribute intensity in the S K-edge spectra. Due to poor overlap $\Phi^5_{\pi^*}$ is effectively nonbonding with respect to its interactions with the sulfonyl moiety. By contrast, $\Phi^4_{\pi^*}$ has a strong influence on the electronic structure of the sulfonyl group, although the influence differs substantially depending on the nature of the SG bond. The energy of the SG_{σ^*} orbital increases from Cl to OH to CH_3, in agreement with expected bond strengths.[10,11] This trend is responsible for the observed differences in the interaction of the $\Phi^4_{\pi^*}$ orbital in compounds **1a**, **2a**, and **3a**. In the case of **1a**, the low-lying SCl_{σ^*} orbital is lowered further through its interaction with the aryl group. The higher energy of SOH_{σ^*} results in somewhat greater mixing with the aryl group, resulting in a highly mixed lowest lying final state in the XAS data. By contrast, the alkyl SC_{σ^*} in **3a** loses its ability to effectively interact with the aryl group due to energetic and overlap considerations. In the absence of any $SG_{\sigma^*}-\Phi^4_{\pi^*}$ interactions another interaction becomes more prominent in **3a**: mixing of aryl with available SO_{π^*} orbitals of the sulfonyl.

It can be argued that the impact of the aryl group could be dominated by inductive rather than orbital mixing. To address this issue we investigated the effect of "turning off" aryl contributions by rotation of the aryl ring with respect

(10) Herron, J. T. In *The Chemistry of Sulphones and Sulphoxides*; Patai, S., Rappoport, Z., Stirling, C. J. M., Eds.; John Wiley & Sons Ltd.: New York, 1988, pp 95−106.
(11) Chatgilialoglu, C. G. D.; Kanabus-Kaminska, J. M.; Lossing, F. P. J. *Chem. Soc., Perkin Trans. 2* **1994**, 357–360. Korth, H. G.; Neville, A. G.; Lusztyk, J. *J. Phys. Chem.* **1990**, *94*, 8835–8839.

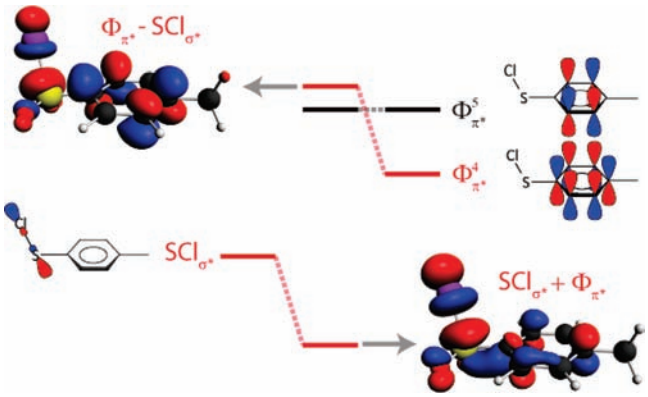

Figure 5. Simplified fragment orbital representation of the hyperconjugation observed between the SCl_{σ^*} and $\Phi^4_{\pi^*}$ orbitals in **1a**. The calculated empty valence MOs resulting from this interaction are shown using an orbital contour isovalue of 0.05 e $Å^{-3}$. The color coding refers to the phase of the calculated MOs.

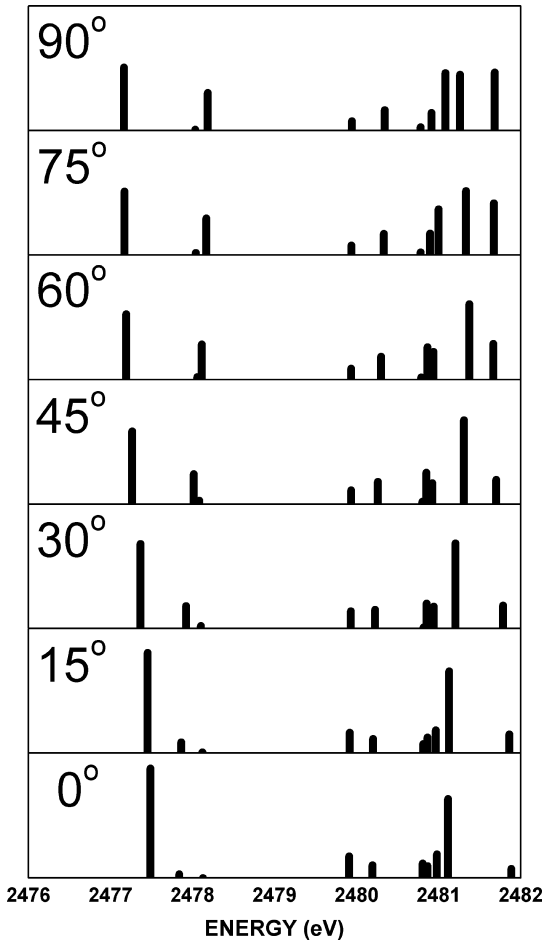

Figure 6. TD-DFT-calculated S K-edge XAS transitions of **1a** as a function of ϕ_{CCSCl} such that $\phi_{CCSCl} = 0°$ corresponds to the S−Cl bond in the plane of the aromatic ring (i.e., no hyperconjugation possible).

to the SG bond. The effect of rotation about the S−C(sp^2) bond on the predicted S K-edge spectrum by TD-DFT is shown in Figure 6. Most importantly, we note that as the aryl group is rotated into proper alignment for direct orbital overlap with the SCl bond, the splitting between the $SCl_{\sigma^*} \leftarrow S_{1s}$ and $\Phi^4_{\pi^*} \leftarrow S_{1s}$ transitions increases by ∼1 eV and the intensity of the latter transition increases at the expense of the former through intensity borrowing. The estimated stabilization of SCl_{σ^*} due to hyperconjugation can thus be estimated to be ∼0.5 eV. Experimentally, the energy difference in the $SCl_{\sigma^*} \leftarrow S_{1s}$ transition on going from **1b** to **1a** is also approximately 0.5 eV.

Observation of the $\Phi^4_{\pi^*} \leftarrow S_{1s}$ transition through intensity borrowing from $SCl_{\sigma^*} \leftarrow S_{1s}$ also allows for an experimental estimate of the magnitude of the hyperconjugative mixing in **1a**. The intensity of the $\Phi^4_{\pi^*} \leftarrow S_{1s}$ transition is a direct result of this mixing, which provides us with an experimentally derived measure of the magnitude of this mixing as given in eq 1. For ToSCl, we therefore estimate 10−15% mixing of the SCl_{σ^*} orbital into the $\Phi^4_{\pi^*}$ (see Figure S11 in the Supporting Information for details). This estimate assumes that the shoulder contains no other contributions, so it should be considered as an upper limit.

$$\%\text{mixing} = \frac{I_{\Phi^4 \leftarrow S_{1s}}}{(I_{\Phi^4 \leftarrow S_{1s}} + I_{SCl_{\sigma^*} \leftarrow S_{1s}})} \times 100\% \qquad (1)$$

Our computational studies further suggest that electronic relaxation plays a role in defining the relative energies of the core transitions investigated. It is the π^* final states of the aryl ring (most specifically $\Phi^4_{\pi^*}$) that are most affected by electronic relaxation. This effect is most dramatically observed in **1a**, where TD-DFT simulations underestimate the splitting of the $SCl_{\sigma^*} \leftarrow S_{1s}$ and $\Phi^4_{\pi^*} \leftarrow S_{1s}$ transitions (1.0 eV by TD-DFT as compared to 2.2 eV experimentally). Estimates for electronic relaxation from ΔSCF calculations indicate that these two transitions behave very differently, resulting in a significant increase in their observed energy splitting. It has been shown previously that electronic relaxation can play a significant role in defining reactivity.[12] In this case, the greater propensity for electronic relaxation in the aryl sulfones correlates with increased pathways for relaxation provided by hyperconjugation.

It is important to note that the effect discussed above is one that involves, in principle, two *empty* valence orbitals and as such does not reflect a typical hyperconjugative effect. The effect of this mixing, however, is extremely important in the photoexcited state that likely dominates photolysis of the S−Cl bond. Scheme 2 indicates that excitation of ToSCl results in a singly occupied SCl_{σ^*}, which should be significantly affected by mixing with the $\Phi^4_{\pi^*}$ orbital. This *excited-state hyperconjugation*[13] should therefore be extremely important in defining the S−Cl bond photocleavage. As observed from the photolysis data, S−Cl photocleavage is more prominent in **1a** than **1b**, in agreement with the postulate that the aryl group should have a large influence on S−Cl bond cleavage. Most importantly, the observed excited-state hyperconjugation of the SCl_{σ^*} orbital with the $\Phi^4_{\pi^*}$ orbital of the aryl group in **1a** allows for partial delocalization of the excited state during photolysis. This

(12) Kennepohl, P.; Solomon, E. I. *Inorg. Chem.* **2003**, *42*, 679–688. Kennepohl, P.; Solomon, E. I. *Inorg. Chem.* **2003**, *42*, 689–695. Kennepohl, P.; Solomon, E. I. *Inorg. Chem.* **2003**, *42*, 696–708.

(13) Rao, C. N. R.; Goldman, G. K.; Balasubramanian, A. *Can. J. Chem.* **1960**, *38*, 2508–13. Wladislaw, B.; Viertler, H.; Olivato, P. R.; Calegao, I. C. C.; Pardini, V. L.; Rittner, R. *J. Chem. Soc., Perkin Trans. 2* **1980**, 453–6. Nakai, H.; Kawai, M. *J. Chem. Phys.* **2000**, *113*, 2168–2174.

delocalization of the SCl_{σ^*} orbital should affect the photochemical process in two distinct ways: (i) it decreases the excitation energy (~0.5 eV) through a combination of orbital mixing and electronic relaxation and (ii) it should increase the excited-state lifetime through charge separation. An increased lifetime of the SCl_{σ^*} excited state would allow for a higher transmission coefficient for the overall reaction and therefore a more efficient overall photocleavage reaction. We are currently exploring these ideas in a series of substituted aryl sulfonyl chlorides to provide further insights into the magnitude of excited-state hyperconjugation in these systems and its importance in defining their photochemistry.

Conclusion

This study provides the first rigorous assignment of the S K-edge XAS spectra for aryl and alkyl sulfonyls, providing clear evidence for the influence of hyperconjugation in aryl sulfonyls. This approach allows for direct measurement of the effect of excited-state hyperconjugation into the SCl_{σ^*} valence orbital, providing the opportunity to explore the importance of this effect in a quantitative manner. Furthermore, it is shown that electronic relaxation is quite substantial in the aryl sulfones, presumably due to the greater excited-state delocalization due to hyperconjugation. This study lays the foundation for the detailed investigation of sulfonyl chlorides and providing a direct experimental measure for hyperconjugation and its influence on reactivity.

Experimental Section

Materials. Polycrystalline powders of *p*-toluene sulfonyl chloride, *p*-toluene sulfonic acid, phenyl ethyl sulfone, methionine sulfone, and methane sulfonate along with a neat solution of methane sulfonyl chloride were purchased from Sigma-Aldrich and stored at 4 °C until use. Sulfur-free Kapton tape was purchased from Creative Global Services Inc. and checked for sulfur contamination (by S K-edge XAS) before use. The irradiation source was a Ushio 75 W xenon Arc Lamp (15023JDHL) purchased from Olis, Inc.

Sample Preparation. Samples were mounted as a finely ground powder dusted on sulfur-free Kapton tape, and spectra were acquired while the samples were irradiated with a 75 W xenon arc lamp at −20 °C under a helium atmosphere with less than 1% oxygen content. The neat solution of methyl sulfonyl chloride was also mounted on the sulfur-free Kapton tape and covered with a polypropylene window. Each scan took 5.5 min.

Data Collection for XAS. XAS data were collected at beamline S06-2 of the Stanford Synchrotron Radiation Laboratory (SSRL) using a modified low Z setup allowing for low-temperature data acquisition and in situ photoirradiation with a 75 W Xe arc lamp. Details of the beamline and data acquisition set are described elsewhere.[14] Energy calibration of the spectra was performed using sodium thiosulfate ($Na_2S_2O_3$) with the first pre-edge feature being calibrated at 2472.02 eV. Calibration scans were performed before and after every data set to ensure stable monochromator readings. Signal was detected with a argon fluorescence (Lytle) detector at ambient temperature and pressure (~1 atm, 298K).[15]Spectra were normalized according to previous published procedures.[16]

DFT Calculations. DFT calculations were carried out using the Amsterdam Density Functional Package Software 2007.01[17] for model compounds of *p*-toluene sulfonyl chloride, *p*-toluene sulfinic acid, ethyl phenyl sulfone, dimethyl sulfone, and methane sulfinic acid. Full geometry optimizations were followed by single-point calculations and time-dependent density functional theory (TD-DFT) using the BP86 (Becke−Perdew 86) functional and a TZ2P basis set with no molecular symmetry. No core for any of the atoms was chosen to allow sulfur core 1s excitation energies for each to be calculated using the ModifyExcitations key (see Supporting Information for input files). The resulting excitation energies for the sulfur 1s electrons were shifted by 77−79 eV to account for computational error in the calculated core excited-state energies. ΔSCF-recalculated transition energies were carried out for the first 10 transitions of each model compound by having 1.5 electrons in the S_{1s} orbital and one-half of an electron in the orbital of interest. A linear transit calculation was carried out for *p*-toluene sulfonyl chloride, and sulfur core 1s excitation energies were calculated for angles of 90°, 75°, 60°, 45°, 15°, and 0° between the S−Cl bond and the plane of the aromatic ring. To help in the assignment of the transitions fragment analysis calculations were carried out on the RSO_2G compounds with R, SO_2, and G as the designated fragments.

Acknowledgment. This research was funded through a Natural Sciences and Engineering Research Council (NSERC, Canada) Discovery Grant to P.K. Infrastructure support was provided by UBC. Special thanks to Dr. Serena DeBeer George at the Stanford Synchrotron Radiation Laboratory (SSRL) for technical and scientific assistance during data collection. Portions of this research were carried out at SSRL, a national user facility operated by Stanford University on behalf of the U.S. DOE-BES. The SSRL Structural Molecular Biology Program is supported by the DOE, Office of Biological and Environmental Research, and the NIH, National Center for Research Resources, Biomedical Technology Program.

Note Added after ASAP Publication. Due to a production error, this article was published ASAP on December 31, 2008, with an incorrect version of Scheme 1. The corrected article was published ASAP on January 8, 2009.

Supporting Information Available: [S1–S6] Input files for TD-DFT XAS simulations, including optimized coordinates. [S7] Sample input file for ΔSCF recalculated transition energies. [S8] Sample input file for fragment analysis used for spectroscopic assignments shown in Tables 1–6. [S9] Linear transit input for **1a**. [S10] Geometry used for compound **3a**. [S11] Details of calculation of percent hyperconjugation. This material is available free of charge via the Internet at http://pubs.acs.org.

IC801665F

(14) Kennepohl, P.; Wasinger, E.; George, S. D. *J. Synchrotron Radiat.* Submitted for publication.

(15) B. Hedman, P. F.; Gheller, S. F.; Roe, A. L.; Newton, W. E.; Hodgson, K. O. *J. Am. Chem. Soc.* **1988**, *110*, 3798. Shadle, S. E.; B., H.; Hodgson, K. O.; Solomon, E. I. *J. Am. Chem. Soc.* **1995**, *117*, 2259.

(16) Delgado-Jaime, M. U.C., J. C.; Fogg, D. E.; Kennepohl, P. *Inorg. Chim. Acta* **2006**, *359*, 3024–3047.

(17) (a) ADF 2007.01, *Theoretical Chemistry*, Vrije Universiteit: Amsterdam, The Netherlands,http://www.scm.com. Guerra, C. F.; Snijders, J. G.; te Velde, G.; Baerends, E. J. *Theor. Chem. Acc.* **1998**, *99*, 391–403. Velde, G. T.; Bickelhaupt, F. M.; Baerends, E. J.; Guerra, C. F.; Van Gisbergen, S. J. A.; Snijders, J. G.; Ziegler, T. *J. Comput. Chem.* **2001**, *22*, 931–967.